MATERIALS SCIENCE

Direct metabolite detection with an n-type accumulation mode organic electrochemical transistor

Anna Maria Pappa[1,2]*, David Ohayon[3]*, Alexander Giovannitti[4]*, Iuliana Petruta Maria[4], Achilleas Savva[3], Ilke Uguz[1†], Jonathan Rivnay[5,6], Iain McCulloch[4,7], Róisín M. Owens[1,2‡], Sahika Inal[3‡]

The inherent specificity and electrochemical reversibility of enzymes poise them as the biorecognition element of choice for a wide range of metabolites. To use enzymes efficiently in biosensors, the redox centers of the protein should have good electrical communication with the transducing electrode, which requires either the use of mediators or tedious biofunctionalization approaches. We report an all-polymer micrometer-scale transistor platform for the detection of lactate, a significant metabolite in cellular metabolic pathways associated with critical health care conditions. The device embodies a new concept in metabolite sensing where we take advantage of the ion-to-electron transducing qualities of an electron-transporting (n-type) organic semiconductor and the inherent amplification properties of an ion-to-electron converting device, the organic electrochemical transistor. The n-type polymer incorporates hydrophilic side chains to enhance ion transport/injection, as well as to facilitate enzyme conjugation. The material is capable of accepting electrons of the enzymatic reaction and acts as a series of redox centers capable of switching between the neutral and reduced state. The result is a fast, selective, and sensitive metabolite sensor. The advantage of this device compared to traditional amperometric sensors is the amplification of the input signal endowed by the electrochemical transistor circuit and the design simplicity obviating the need for a reference electrode. The combination of redox enzymes and electron-transporting polymers will open up an avenue not only for the field of biosensors but also for the development of enzyme-based electrocatalytic energy generation/storage devices.

INTRODUCTION

Enzyme-based electrocatalysis has gained significant interest for the development not only of energy conversion devices but also of biosensors (*1*). The inherent substrate specificity and catalytic activity of enzymes (oxidoreductases) coupled with their ability to undergo electronic communication with the sensing electrode have stimulated their widespread application in amperometric biosensors, predominantly for the detection of physiologically relevant metabolites such as glucose (*2*). An obvious prerequisite when it comes to engineering such bioelectrochemical devices is the electron transfer (ET) between the sensing electrode and the redox active sites of the enzyme. For most of the enzymes, efficient electrical communication with the electrode is largely restricted by the distance between the active sites (and/or the electron transport pathways within the enzyme) and the electrode surface (*3*, *4*). This is more of an issue for flat, unstructured surfaces of traditional electrode materials, limiting intermolecular interactions. To mediate ET, a typical strategy has, therefore, been the inclusion of redox active molecules acting as electron relays in the sensor architecture—in a freely diffusing form or coupled to the electrode (*5*).

Organic mixed conductors (OMCs) are often conjugated polymers that support electronic charge transport along their backbones, while allowing for ionic transport through their bulk (*6*), with great potential to act as electron relays. Alongside their inherent ability to undergo reversible electrochemical reactions, their fuzzy/soft surfaces can aid in promoting interactions with proteins, thus inducing electronic communication with the catalytic sites of the enzymes (*5*, *7*–*12*). In addition, OMCs enable different modes of device operations, a state-of-the-art example being the organic electrochemical transistor (OECT). As an electrolyte-gated transistor, the OECT can transduce ionic signals of biological origin into electronic ones (*13*–*15*), with particularly high amplification. This is due to the volumetric interactions of the electrolyte (dopant/dedopant) ions with the bulk of the OMC channel (*16*), leading to remarkable sensitivity for biotransduction (*17*, *18*). We have recently shown OECTs composed of the p-type semiconductor poly(3,4-ethylenedioxythiophene) doped with polystyrenesulfonate (PEDOT:PSS) and coupled with the corresponding oxidase enzymes for metabolite sensing (*19*, *20*). By making an array of such microfabricated devices, we could detect multiple disease-related metabolites from one drop of human saliva with remarkable specificity (*19*), and more recently, minute changes in the concentration of lactate secreted from tumor cells in vitro could be monitored by incorporating reference-based circuits (*20*).

In the aforementioned OECTs, however, as in most electrochemical biosensors to date, direct ET has been rather sluggish, limiting their selectivity and speed. This can be overcome by the integration of ET mediators, albeit at the expense of complicating the sensor fabrication. Moreover, despite the high signal amplification provided by the OECT, PEDOT:PSS-based devices display the inherent disadvantage in that they operate in depletion mode. In this regime, electrochemical

[1]Department of Bioelectronics, École Nationale Supérieure des Mines, Centre Microélectronique de Provence, Gardanne 13541, France. [2]Department of Chemical Engineering and Biotechnology, University of Cambridge, Philippa Fawcett Drive, Cambridge CB3 0AS, UK. [3]Biological and Environmental Sciences and Engineering Division, King Abdullah University of Science and Technology (KAUST), Thuwal 23955-6900, Kingdom of Saudi Arabia. [4]Department of Chemistry and Centre for Plastic Electronics, Imperial College London, London SW7 2AZ, UK. [5]Department of Biomedical Engineering, Northwestern University, 2145 Sheridan Road, Evanston, IL 60208, USA. [6]Simpson Querrey Institute for BioNanotechnology, Northwestern University, Chicago, IL 60611, USA. [7]Physical Science and Engineering Division, KAUST, Thuwal 23955-6900, Kingdom of Saudi Arabia.
*These authors contributed equally to this work.
†Present address: Department of Electrical Engineering, Columbia University, New York, NY 10027, USA.
‡Corresponding author. Email: rmo37@cam.ac.uk (R.M.O.); sahika.inal@kaust.edu.sa (S.I.)

dedoping of the p-type channel (that is, a decrease in its conductance) as a result of the applied gate potential or a biological event (such as the enzyme-based electrocatalysis) will switch the transistor off. For biosensing, however, it is more advantageous to have an accumulation mode device (*21*), which switches on upon the biorecognition event as in depletion mode sensors; a reduction in current over time, possibly due to degradation of the polymer, might intervene with the actual sensor output. Moreover, the depletion OECT being always on has adverse influence on power consumption. While the inherent specificity and electrochemical reversibility of enzymes poise them as the biorecognition element of choice for a wide range of metabolites, challenges associated with their facile integration and efficient communication with electrodes remain. With the notable exception of today's market praised success story in glucose biosensors, enzyme-based devices, including OECTs, are still limited in their adaptation into different geometries and form factors and for applications beyond in vitro platforms.

RESULTS

n-Type OECTs for direct detection of lactate

Addressing these mutually stringent requirements in material and device design for enzymatic sensing of metabolites, we report the use of an n-type mixed conductor in an accumulation mode OECT for the detection of lactate. The n-type–conjugated polymer that we chose as the active material is based on an NDI-T2 copolymer (*22*), which has a backbone comprising a highly electron-deficient naphthalene-1,4,5,8-tetracarboxylic diimide (NDI) repeat unit and an electron-rich unsubstituted bithiophene repeat unit (T2), hereinafter called P-90 (Fig. 1A). The side chains on the diimide unit were a 90:10 randomly distributed ratio of polar glycol and nonpolar branched alkyl groups, where the ratio was optimized to ensure solubility of the copolymer in polar solvents (*23*). The glycol side chains are envisaged to serve the dual role of (i) providing polar groups for the enzyme to interact with (*24*) and (ii) enhancing the polymer's water uptake capacity (*25*), known to promote electrochemical activity in aqueous media (*15*).

The copolymer P-90–based OECT coupled with lactate oxidase (LOx) is schematically depicted in Fig. 1B. We adopted an all-planar configuration where we use the polymer in the channel and at the gate electrode. Note that the film surface is not chemically treated to immobilize the enzyme (the enzyme solution was simply placed on the active area), neither is an ET mediator incorporated into our system. As such, the device not only is compatible with large area processes such as printing but also provides ease of integration with microfluidics or adaptation for use in in vivo environments (*26*). These accumulation mode OECTs exhibit a high signal on/off response (translating into high gain) and a low-power operation in common aqueous electrolytes (*27*). The current-voltage characteristics show a monotonic increase of the source-drain current (I_D) with increasing gate voltage (V_G) due to doping of the film by the cations injected from the phosphate-buffered saline (PBS), a buffer that mimics the pH, osmolarity, and ion concentration in the human body (fig. S1). The first derivative of this curve, that is, the output (I_D) of the

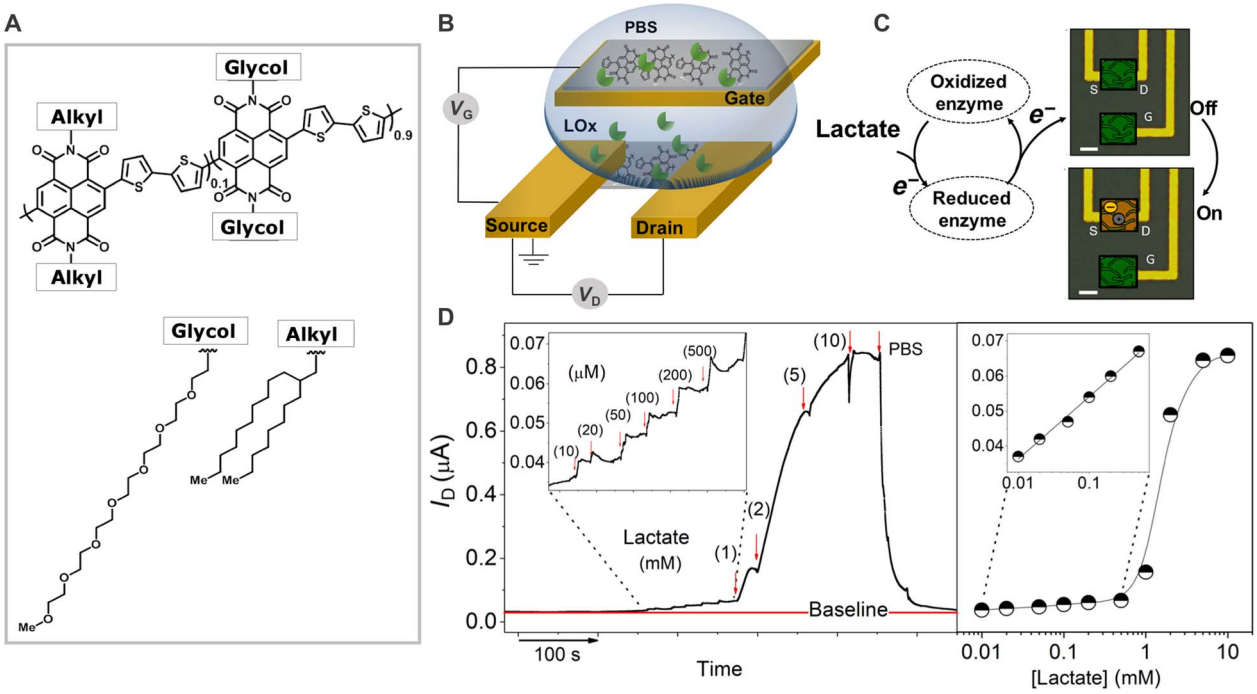

Fig. 1. Mediator and reference electrode–free sensing of lactate with an accumulation mode OECT based on an n-type OMC. (**A**) Chemical structure of the n-type copolymer P-90. (**B**) Schematic of the OECT [gate dimensions, 500 μm^2; channel dimensions, 10 μm (length) × 100 μm (width) × ~100 nm (thickness)]. (**C**) Schematic of the OECT biosensor showing the presumed interactions between the enzyme, LOx, and the n-type channel (note also that the gate electrode is exposed to LOx and lactate). (**D**) Real-time response of the OECT (source-drain current, I_D, as a function of time) as successive amounts of lactate are added to the PBS solution containing the enzyme, LOx, and the corresponding calibration curve in semilogarithmic scale. Arrows indicate the addition of lactate. After 10 mM lactate, the device is washed with PBS, and the output signal decreases back to its initial value. The insets represent the magnified response of the transistor to low amounts of the analyte (10 to 500 μM).

device versus the input (V_G), expresses the signal amplification by the OECT, namely, the transconductance. The transconductance curve follows a monotonic trend as well: The efficiency of transduction scales with V_G (fig. S1B). Giovannitti and co-workers (*28*) recently showed that the polar glycol side chains attached to such hydrophobic polymer backbones enabled reversible electrochemical switching between the reduced (n-type–doped), oxidized (p-type–doped), and neutral state of the film in similar aqueous electrolytes. During the reduction process (triggered by a positive gate bias), cations drift into the film to counterbalance the electrons stabilized on the backbone of the copolymer.

As P-90 has the ability to stabilize electrons on its backbone, those generated during an enzymatic reaction could be directly transferred to the channel, increasing its conductivity (*29*), thereby turning the device on (Fig. 1C). Figure 1D shows the chronoamperometric response of the OECT, that is, the change in the saturation current that flows through the P-90 channel, to the real-time additions of cumulative concentrations of lactate in the presence of LOx in PBS. The I_D increases with increasing concentrations of lactate, suggesting a reaction-triggered gating of the channel. The specific and reversible reaction of LOx with lactate affects the conductance of the channel. We note that the device is responsive to lactate only when it is operated at gate voltages equal to or higher than the threshold voltage (that is, the minimum V_G required to turn the device on) (fig. S2). The dose-dependent effect of lactate on the steady-state characteristics of the OECT, for a remarkably wide range of concentrations, outperforms PEDOT:PSS-based OECTs of comparable geometry used as lactate sensors, despite the absence of an electron mediator (*19*). Our platform yields excellent biosensor analytical characteristics as evidenced from the normalized lactate titration curves (fig. S3). When operated in the bespoke parameters (that is, V_D = 0.7 V and V_G = 0.5 V), the channel with this particular geometry responds to micromolar concentrations of lactate with a linear relationship up to 1 mM and a wide dynamic range of detection from 10 μM to 10 mM. The change in the I_D occurs rapidly (within ca. 2 s), particularly for low metabolite concentrations (<0.3 mM) (Fig. 1D). Notably, the device response is reversible; for example, when the 10 mM lactate solution on top of the device is replaced with PBS (washing step), the current reverts to its initial, lactate-free value. The device response to lactate is reproducible with no significant device-to-device and measurement-to-measurement variations, especially for the detection of low lactate concentrations (mean calculated error, 2.4%; fig. S3).

Detection mechanism

To elucidate the mechanism behind the gradual increase in the channel current as lactate is oxidized by LOx in the electrolyte, we sought to gain insights into the interactions between the enzyme and the film, which will most likely lead to such an efficient electrochemical communication. We used quartz crystal microbalance with dissipation monitoring (QCM-D) measurements because of the versatility of the tool in monitoring interactions of a solid surface with certain species in a solution (*30*). Figure 2A shows the enzyme-induced changes in the oscillation frequency of the QCM crystal coated with the copolymer P-90 that are translated into the variations in the mass of the film (see fig. S4 for the raw QCM-D data, that is, frequency change versus time plots). As LOx is introduced into the PBS solution that is flowing over the film, the mass on the sensor increases (Fig. 2A, the region marked as "+LOx"). We also monitor distinct changes in the surface topography of the polymer film in the presence of the enzyme [compare the atomic force microscopy (AFM) images on the left and in the middle of the inset of Fig. 2A and fig. S5, B and C]. Even after rinsing this film with PBS, we find that a high amount of the enzyme remains on the polymer surface (Fig. 2A, the region marked as "Rinse"). At this stage, the film surface is also rougher compared to its pristine state, which further substantiates the localization of the protein on the surface (the AFM image on the right of the inset of Fig. 2A; see also fig. S5, A and D).

The cyclic voltammetry (CV) curves show footprints of the interactions and the electronic communication between the enzyme and the film (Fig. 2B, compare PBS; P-90 only, with +LOx; upon enzyme addition). The CV curve of P-90 in PBS is characterized by two reversible redox couples (fig. S6A). The associated redox peaks are attributed to ET processes along the chain where the negative charge is mainly localized on the carbonyl oxygens of the NDI unit (*31*). The enzyme addition causes an increase both in the reduction and in the oxidation peak currents—we do not observe new features possibly due to the inherently complex CV curve of P-90—while the oxidation peak shifts slightly toward more positive voltages (Fig. 2B and fig. S6A). The increase in the redox peak amplitudes can be attributed to the activity of flavin mononucleotide (FMN), the catalytic site of LOx (*32*, *33*). When lactate is added into the solution and is oxidized by LOx, we observe an increase in the cathodic current, as well as a shift of the peak potentials, which is more prominent as the lactate concentration increases (Fig. 2B). The electrocatalytic reactions occurring during the enzymatic sensing of lactate are described in fig. S6B (*4*). These changes can be related to a local pH decrease, resulting from the H^+ produced upon the enzymatic reaction and/or because of the high amount of lactate present in the solution (see fig. S7A for the pH of the solution in the presence of enzymatic reactions with different amounts of lactate). We therefore investigated the net effect of pH on the electrochemical behavior of the P-90 film (fig. S7B). With the decrease of solution pH from 7.4. to 5, both the cathodic and anodic peak potentials shift slightly toward positive potentials, accompanied by a decrease in their magnitudes. Only below pH 4 do we see an increase in the peak amplitudes, suggesting the participation of H^+ to dope the polymer. We therefore conclude that H^+ evolution in the solution seems to be responsible for the shift of the redox peak potentials but does not play a major role in generating current, at least for lactate concentrations below 15 mM (pH <4). As such, the observed changes in the CV curve of P-90 in Fig. 2B can be attributed to a synergistic effect of ET and a local pH decrease, while the contribution of the latter is pronounced for high lactate concentrations.

The ultraviolet–visible–near-infrared (UV-VIS-NIR) absorbance spectrum of the P-90 film in PBS solution containing LOx illustrates these interactions from another aspect (Fig. 2C). The changes in the spectrum that occur upon enzymatic reaction are comparable to those observed when the film is electrochemically doped by electrolyte cations (fig. S8). When lactate is added to the solution containing LOx, the absorbance peaks between 350 and 550 nm increase in intensity, with a subsequent decrease in the broader energy transition between 550 and 850 nm, which is attributed to an intramolecular charge transfer complex. These spectral changes suggest doping of the polymer film upon enzymatic reaction. The electrons produced in the reaction are efficiently transferred to the conjugated backbone, increasing the charge carrier density and hence the conductivity of the copolymer, even at voltages as low as −0.1 V (versus Ag/AgCl), which is below the reduction peak of the copolymer (Fig. 2D). It is worthy to note that, in response to 10 mM lactate, the OECT channel generates three

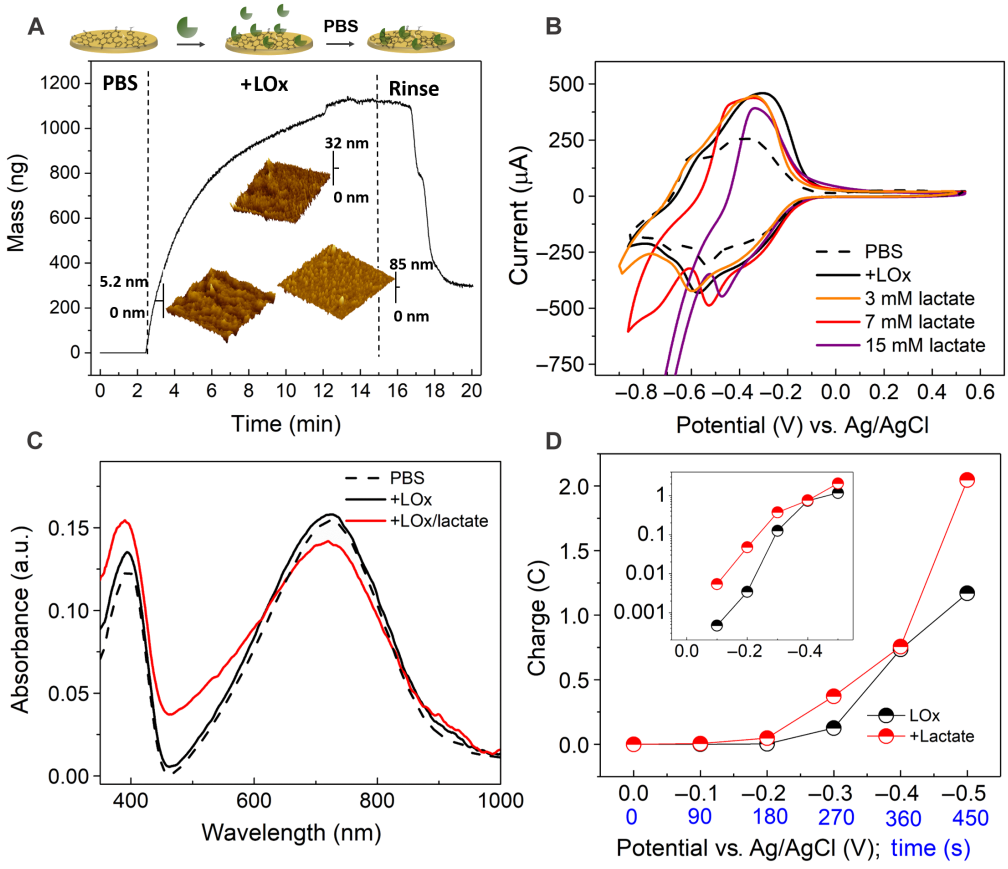

Fig. 2. Investigating the interactions between the n-type polymer and the enzyme, which lead to efficient electrical communication. (**A**) QCM-D measurements showing the interactions between the enzyme and the polymer film in three stages: when the film is exposed to the electrolyte (PBS), when the enzyme is injected into the PBS solution (+LOx), and when the enzyme-exposed film is rinsed with PBS (Rinse). The mass of the film was calculated using a viscoelastic model. Three-dimensional AFM images (2 × 2 μm^2) show the changes on the surface of the film during the three stages. (**B**) CV curve of the P-90 film cast on gold (Au)–coated glass substrate recorded in PBS (dashed black lines) and with LOx (black solid lines). The spectrum changes further upon addition of increasing concentrations of lactate into the solution because of the reaction with LOx. The scan rate is 50 mV s^{-1}. (**C**) The changes in the UV-VIS-NIR spectrum of the P-90 film, cast on an indium tin oxide (ITO) substrate, in PBS solution containing the enzyme (black curve) and upon addition of 10 mM lactate (red curve). The curves are normalized to the absorbance value at 1000 nm where no changes occur during electrochemical switching (fig. S8). a.u., arbitrary units. (**D**) The number of charges generated by this film while a reduction potential (−0.5 V) was applied using an Ag/AgCl electrode immersed in the same solution as in (C). The red curve represents the current generated in the co-presence of lactate and LOx in the solution. The inset shows the same plot, this time in semilogarithmic scale, magnifying the current generated at low voltages.

orders of magnitude higher current density compared to the output of this macroscale electrode (biased at −0.5 V with respect to the reference electrode), highlighting the gain that the transistor circuit provides.

Generally, for oxidases (such as LOx) where the cofactor is not sufficiently wired to the electrode and in the absence of an ET mediator, the diffusing molecular O_2 sequesters the electrons from the reduced cofactor and is converted to hydrogen peroxide (H_2O_2) (fig. S6B) (*5*). To rule out the possibility of P-90 exhibiting inherent catalytic activity toward H_2O_2, we tested the device sensitivity to H_2O_2. Figure 3A shows the device response to cumulative concentrations of H_2O_2, corresponding to the lactate concentrations tested in this study. The negligible change in channel conductance with H_2O_2 further confirms the selectivity of the sensor to lactate and that the ET from the enzyme to the film governs the device operation. Likewise, we find no significant differences in the electrochemical behavior of the system recorded in air-saturated PBS compared to that in deoxygenated PBS (fig. S9). In air, only slightly higher reduction (and oxidation) currents can be observed because of the diffusing O_2 that acts as an electron acceptor competing with P-90. Moreover, the sensitivity of the device to detect lactate is specific to its oxidation by the enzyme and not due to a decrease in pH of the solution (for example, H^+ doping). The decrease in solution pH, adjusted via HCl additions or an increase in lactate concentration, does not have a major influence in the normalized response (NR) of the OECT (see the inset of Fig. 3A and fig. S10A). Together, we conclude that the enzyme is efficiently anchored to the surface of the P-90 film, presumably because of interactions with ethylene glycol side chains (*24*). As such, it has a good electrochemical contact with the redox-active copolymer; that is, the electrons generated from the enzymatic reaction can be transferred from the FMN to the polymer backbone (Fig. 3B). The NDI units of the copolymer act not only as electron-transporting conjugated segments but also as redox centers, capable of switching between the neutral and reduced state, thus obviating the need for a mediator (*34*).

Controlling the analytical characteristics of the sensor

In the comparative lactate titration curves of the n-type accumulation mode OECT biosensor, we show how the analytical characteristics of

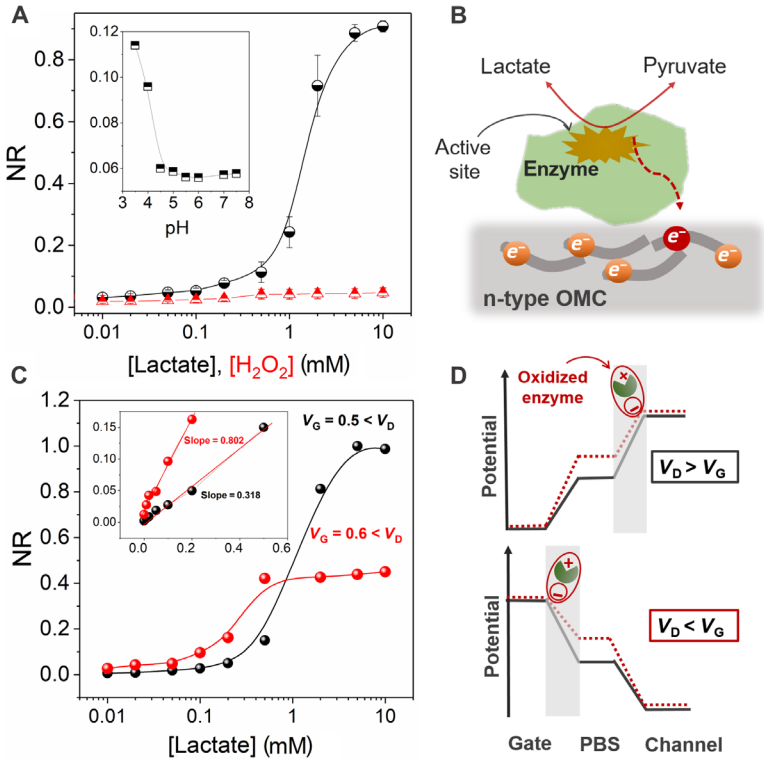

Fig. 3. Elucidating the sensing mechanism and control over the sensor performance. (**A**) NR of the OECT to H_2O_2 (red triangles) and to lactate in the presence of LOx (black circles). The inset shows the sensitivity of the device to pH. The pH was adjusted using HCl and measured with an external pH electrode. The plot shows that the sensor cannot catalyze H_2O_2 oxidation and exhibits negligible response to changes in pH. Error bars represent the SD from four measurements on two devices. (**B**) The proposed mechanism of lactate sensing based on the direct ET from the enzyme to the n-type OMC. (**C**) Normalized calibration curves of the device operated under different biasing conditions at the gate electrode for a V_D fixed at 0.7 V. The inset shows the response of the device to lactate, this time represented in linear scale, with the slope indicating the sensitivity of the device. (**D**) The distribution of electrolyte potential at the critical interfaces (gate/electrolyte and channel/electrolyte) in the presence of the enzymatic reaction under different relative biasing conditions.

the sensor change depending on the biasing conditions (Fig. 3C). At a higher gate bias (V_G = 0.6 V compared to 0.5 V), the sensor exhibits better sensitivity at the low lactate concentration regime (<1 mM) as determined from the slope of the linear calibration curve (Fig. 3C, inset). The increased sensitivity at higher gate bias can be sought to be directly correlated to the device's transconductance. At a V_G of 0.6 V, the transconductance of the device is higher compared to operation at V_G = 0.5 V (fig. S1B). However, operating the device at high V_G leads to faster saturation; that is, the sensor is no longer responsive to high concentrations of lactate (>0.5 mM). The closer to the threshold potential the device is gated, the larger the operation window, and therefore the larger the dynamic range of the sensor. Thus, by adjusting the gate potential, one can tune the sensitivity of the biosensor to the desired lactate concentration range, depending on the application demands. Another striking feature of this device type is the capability to drive the enzymatic reaction either at the gate or at the channel by varying the magnitude of the voltage applied at the corresponding contacts (Fig. 3D). This is implausible with the benchmark OECTs based on the p-type PEDOT:PSS because the oxidation reaction always takes place at the positively biased gate electrode rather than the negatively biased channel. When $V_G > V_D$, the gate acts as the oxidizing electrode, while the channel amplifies the sensing event (fig. S10B). The ability to tune the polarity of the two electrodes can be beneficial in cases where the potential drop is equal at the two interfaces; that is, the gate and the channel have the same size and are made of the same material.

DISCUSSION

Our device embodies a new concept in enzyme-based sensing where we take advantage of the superior ion-to-electron transducing qualities of an electron-transporting (n-type) organic semiconductor and the inherent amplification properties of an ion-to-electron converting device, the OECT. We demonstrate the detection of lactate, a target metabolite of high biological significance in determining cellular metabolic pathways and tightly associated with critical health care conditions, using a fully integrated, miniaturized, easy-to-fabricate all-polymer transistor platform. We postulate that the polar side chains of the copolymer aid in promoting interactions with the enzyme, alleviating the need of synthetic or post-synthesis biofunctionalization approaches that aim to bring the enzyme in close proximity to the sensing surface. As such, direct electrical communication between the film and the enzyme enables mediator-free direct detection of lactate, benefiting from the electron-accepting properties of the OMC. When used in an OECT configuration, the sensing performance is greatly enhanced because of the inherent amplification of these devices.

To achieve a reliable performance in real-world applications, however, we need to consider several factors. The observed deviation in the sensor performance among different devices is mostly attributed to the thickness variations of the film in the channel, which affect the gain of the OECT. We believe that control over film thickness can be easily addressed by adjusting the fabrication procedure as we showed in our previous study (*20*). Furthermore, the error arising from multiple

measurements on the same device can be reduced by introducing a more controlled environment for the addition of lactate. For example, the volume of the liquid that the device is exposed to could be controlled precisely by integration of microfluidics, which would mitigate user error.

One obvious advantage of this accumulation mode OECT compared to a conventional amperometric sensor is the inherent amplification of the signal by the channel, allowing for miniaturization. Only a few tens of micromolars of lactate causes a detectable change in the channel current. When the micrometer-scale LOx-functionalized channel is used as a resistor (simply by disconnecting the gate electrode), the change in its current with lactate is close to noise level, highlighting the role of the transistor circuit in amplifying the signal. The use of a lateral micrometer-scale gate electrode based on the n-type polymer and elimination of an external reference electrode allow for straightforward adaptation of this device type into different geometries and forms and, thus, greatly expand the application scope. Furthermore, we showed that by controlling the operation conditions, we could not only fine-tune the sensor's analytical performance but also determine where the redox reactions take place, without the need to redesign de novo. One evident benefit of this mode of operation is its compatibility with spatially resolved multiparametric sensing based on a single device platform including a common gate electrode and channels functionalized with different enzymes.

This is the first demonstration of an accumulation mode OECT for biosensing and the use of n-type polymers in enzymatic sensing. The functionalization is simple, and the device design is elegant, obviating the need for mediators and a reference electrode. The role of OECT as both the amplifier and transducer and the design simplicity endowed by the inherent surface and bulk properties of the n-type material poise the resulting platform as a prominent alternative to the conventional amperometric enzyme electrodes. We further anticipate that this combination of redox enzymes with n-type polymers will open up an avenue not only for the field of biosensors but also for the development enzyme-based electrocatalytic energy generation/storage devices.

MATERIALS AND METHODS

Device fabrication

For the device fabrication, the Au contacts (located at the source, drain, and gate) and interconnects were patterned on a glass substrate, and an additional layer of Parylene C was used to insulate the Au interconnects according to established protocol (*27*). The final channel dimension is 10 μm in length and 100 μm in width, while the gate electrode has an active area of 500 μm^2. The active material, P-90, was spin-cast directly from a solution (1000 rpm, 30 s) without any annealing or postprocessing steps. The polymer P-90 was synthesized according to the literature (*23*).

Film characterization

All characterization was performed in PBS. The cyclic voltammograms were recorded using a potentiostat-galvanostat (PGSTAT128N, Autolab) with an Ag/AgCl reference electrode and a Pt counter electrode. The working electrode was P-90 cast on a Au-coated glass substrate. The system, in a closed chamber, was systematically degassed for at least 15 min in N_2 before performing any measurements for characterization under inert atmosphere. The topography and the roughness of the polymer film and the enzyme adsorption were investigated using AFM and QCM-D. AFM measurements were performed in tapping contact mode with an Agilent 5500 SPM AFM in both air and liquid. QCM-D measurements were conducted using a Q-sense analyzer (QE401) on a bare Au sensor (as reference) and then on the Au sensor coated with the film. The data were treated with a viscoelastic model to calculate the mass of the enzyme adsorbed on the film (*35*). UV-VIS-NIR spectra were recorded using an Ocean Optics QE Pro Scientific grade spectrometer (185 to 1050 nm). For spectroelectrochemistry measurements, the spectrometer was coupled to a Keithley 2606A source measure unit, and when required, bias was applied between the polymer-coated ITO substrate, which serves as the working electrode and a Ag/AgCl reference electrode.

Chronoamperometric lactate sensing measurements

For the sensing experiments, LOx in PBS (10 mg ml^{-1}) was drop-casted on the device active area (channel and gate). The schematics describing this functionalization step can be found in Fig. 2A. Lactate was dissolved as stock solutions in PBS. Current-voltage characteristics of the devices were recorded using a Keithley 2612A dual SourceMeter. The readout signal of the OECT at zero analyte concentration was the steady-state current obtained in PBS solution. After a steady baseline was obtained for the drain current, changes in response to subsequent additions of increasing concentrations of lactate solutions into the electrolyte were monitored as a function of time. For all the experiments, the volume of the solution was kept fixed at 50 μl. The response of the device to lactate was normalized to allow for an accurate comparison between different devices. The NR was determined by the following equation, which considers the current output after it reaches a steady-state value

$$\mathrm{NR} = \left| \frac{I}{I_{\max}} \right|$$

where I and I_{max} are the current output at a given analyte concentration and the maximum current output of the device at the maximum applied gate potential in the absence of the analyte, respectively.

SUPPLEMENTARY MATERIALS

Supplementary material for this article is available at http://advances.sciencemag.org/cgi/content/full/4/6/eaat0911/DC1

fig. S1. The output and transfer characteristics of a typical all n-type polymer (P-90)–based OECT.
fig. S2. Transfer curves of the OECT in the absence and presence of the enzymatic reaction.
fig. S3. Calibration curve relating the NR of the device to a range of lactate concentrations.
fig. S4. QCM-D response of the P-90–coated sensor immersed in PBS.
fig. S5. AFM topography images of the P-90 film coated on Au substrate.
fig. S6. The CV curve of the P-90 film before and after addition of the enzyme into the PBS solution and a scheme of bioelectrocatalytic reactions.
fig. S7. The effect of pH on the CV curve of the P-90 film.
fig. S8. The changes in the absorbance spectrum of the P-90 film during the electrochemical switch.
fig. S9. The effect of air on the reaction of lactate with LOx-functionalized P-90.
fig. S10. Sensitivity of the device to lactate and when operated under different biasing conditions at the channel and the gate.

REFERENCES AND NOTES

1. A. N. Sekretaryova, M. Eriksson, A. P. F. Turner, Bioelectrocatalytic systems for health applications. *Biotechnol. Adv.* **34**, 177–197 (2016).
2. H. Jiang, Z. Zhao, Enzyme-based electrochemical biosensors, in *Biosensors*, P. A. Serra, Ed. (InTech, 2010).

3. A. P. F. Turner, Biosensors: Sense and sensibility. *Chem. Soc. Rev.* **42**, 3184–3196 (2013).
4. R. S. Freire, C. A. Pessoa, L. D. Mello, L. T. Kubota, Direct electron transfer: An approach for electrochemical biosensors with higher selectivity and sensitivity. *J. Braz. Chem. Soc.* **14**, 230–243 (2003).
5. A.-M. Pappa, O Parlak, G Scheiblin, P Mailley, A Salleo, RM. Owens, Organic electronics for point-of-care metabolite monitoring. *Trends Biotechnol.* **36**, 45–59 (2017).
6. S. Inal, G. G. Malliaras, J. Rivnay, Benchmarking organic mixed conductors for transistors. *Nat. Commun.* **8**, 1767 (2017).
7. B. C. Thompson, O. Winther-Jensen, J. Vongsvivut, B. Winther-Jensen, D. R. MacFarlane, Conducting polymer enzyme alloys: Electromaterials exhibiting direct electron transfer. *Macromol. Rapid Commun.* **31**, 1293–1297 (2010).
8. A. Kros, S. W. F. M. van Hövell, N. A. J. M. Sommerdijk, R. J. M. Nolte, Poly(3,4-ethylenedioxythiophene)-based glucose biosensors. *Adv. Mater.* **13**, 1555–1557 (2001).
9. D. T. Simon, E. O. Gabrielsson, K. Tybrandt, M. Berggren, Organic bioelectronics: Bridging the signaling gap between biology and technology. *Chem. Rev.* **116**, 13009–13041 (2016).
10. P. N. Bartlett, P. R. Birkin, Enzyme switch responsive to glucose. *Anal. Chem.* **65**, 1118–1119 (1993).
11. P.-C. Nien, M.-C. Huang, F.-Y. Chang, K.-C. Ho, Integrating an enzyme-entrapped conducting polymer electrode and a prereactor in a microfluidic system for sensing glucose. *Electroanalysis* **20**, 635–642 (2008).
12. W. Schuhmann, Electron-transfer pathways in amperometric biosensors. Ferrocene-modified enzymes entrapped in conducting-polymer layers. *Biosens. Bioelectron.* **10**, 181–193 (1995).
13. L. Kergoat, B. Piro, M. Berggren, G. Horowitz, M.-C. Pham, Advances in organic transistor-based biosensors: From organic electrochemical transistors to electrolyte-gated organic field-effect transistors. *Anal. Bioanal. Chem.* **402**, 1813–1826 (2012).
14. J. Rivnay, S. Inal, A. Salleo, R. M. Owens, M. Berggren, G. G. Malliaras, Organic electrochemical transistors. *Nat. Rev. Mater.* **3**, 17086 (2018).
15. A. Giovannitti, D. T. Sbircea, S. Inal, C. B. Nielsen, E. Bandiello, D. A. Hanifi, M. Sessolo, G. G. Malliaras, I. McCulloch, J. Rivnay, Controlling the mode of operation of organic transistors through side-chain engineering. *Proc. Natl. Acad. Sci. U.S.A.* **113**, 12017–12022 (2016).
16. J. Rivnay, P. Leleux, M. Ferro, M. Sessolo, A. Williamson, D. A. Koutsouras, D. Khodagholy, M. Ramuz, X. Strakosas, R. M. Owens, C. Benar, J.-M. Badier, C. Bernard, G. G. Malliaras, High-performance transistors for bioelectronics through tuning of channel thickness. *Sci. Adv.* **1**, e1400251 (2015).
17. L. Zhang, G. Wang, D. Wu, C. Xiong, L. Zheng, Y. Ding, H. Lu, G. Zhang, L. Qiu, Highly selective and sensitive sensor based on an organic electrochemical transistor for the detection of ascorbic acid. *Biosens. Bioelectron.* **100**, 235–241 (2018).
18. C. Liao, M. Zhang, M. Y. Yao, T. Hua, L. Li, F. Yan, Flexible organic electronics in biology: Materials and devices. *Adv. Mater.* **27**, 7493–7527 (2015).
19. A.-M. Pappa, V. F. Curto, M. Braendlein, X. Strakosas, M. J. Donahue, M. Fiocchi, G. G. Malliaras, R. M. Owens, Organic transistor arrays integrated with finger-powered microfluidics for multianalyte saliva testing. *Adv. Healthc. Mater.* **5**, 2295–2302 (2016).
20. M. Braendlein, A.-M. Pappa, M. Ferro, A. Lopresti, C. Acquaviva, E. Mamessier, G. G. Malliaras, R. M. Owens, Lactate detection in tumor cell cultures using organic transistor circuits. *Adv. Mater.* **29**, 1605744 (2017).
21. S. Inal, J. Rivnay, P. Leleux, M. Ferro, M. Ramuz, J. C. Brendel, M. M. Schmidt, M. Thelakkat, G. G. Malliaras, A high transconductance accumulation mode electrochemical transistor. *Adv. Mater.* **26**, 7450–7455 (2014).
22. Z. Chen, Y. Zheng, H. Yan, A. Facchetti, Naphthalenedicarboximide- vs perylenedicarboximide-based copolymers. Synthesis and semiconducting properties in bottom-gate N-channel organic transistors. *J. Am. Chem. Soc.* **131**, 8–9 (2009).
23. A. Giovannitti, I. P. Maria, D. Hanifi, M. J. Donahue, D. Bryant, K. J. Barth, B. E. Makdah, A. Savva, D. Moia, M. Zetek, P. R. F. Barnes, O. G. Reid, S. Inal, G. Rumbles, G. G. Malliaras, J. Nelson, J. Rivnay, I. McCulloch, The role of the side chain on the performance of N-type conjugated polymers in aqueous electrolytes. *Chem. Mater.* **30**, 2945–2953 (2018).
24. A. Al-Ani, H. Pingle, N. P. Reynolds, P.-Y. Wang, P. Kingshott, Tuning the density of poly(ethylene glycol) chains to control mammalian cell and bacterial attachment. *Polymers* **9**, 343 (2017).
25. S.-J. Yang, W. Jang, C. Lee, Y. G. Shul, H. Han, The effect of crosslinked networks with poly(ethylene glycol) on sulfonated polyimide for polymer electrolyte membrane fuel cell. *J. Polym. Sci. B Polym. Phys.* **43**, 1455–1464 (2005).
26. D. Khodagholy, T. Doublet, P. Quilichini, M. Gurfinkel, P. Leleux, A. Ghestem, E. Ismailova, T. Hervé, S. Sanaur, C. Bernard, G. G. Malliaras, In vivo recordings of brain activity using organic transistors. *Nat. Commun.* **4**, 1575 (2013).
27. C. B. Nielsen, A. Giovannitti, D.-T. Sbircea, E. Bandiello, M. R. Niazi, D. A. Hanifi, M. Sessolo, A. Amassian, G. G. Malliaras, J. Rivnay, I. McCulloch, Molecular design of semiconducting polymers for high-performance organic electrochemical transistors. *J. Am. Chem. Soc.* **138**, 10252–10259 (2016).
28. A. Giovannitti, C. B. Nielsen, D.-T. Sbircea, S. Inal, M. Donahue, M. R. Niazi, D. A. Hanifi, A. Amassian, G. G. Malliaras, J. Rivnay, I. McCulloch, N-type organic electrochemical transistors with stability in water. *Nat. Commun.* **7**, 13066 (2016).
29. Y. Liang, Z. Chen, Y. Jing, Y. Rong, A. Facchetti, Y. Yao, Heavily n-dopable π-conjugated redox polymers with ultrafast energy storage capability. *J. Am. Chem. Soc.* **137**, 4956–4959 (2015).
30. A.-M. Pappa, S. Inal, K. Roy, Y. Zhang, C. Pitsalidis, A. Hama, J. Pas, G. G. Malliaras, R. M. Owens, Polyelectrolyte layer-by-layer assembly on organic electrochemical transistors. *ACS Appl. Mater. Interfaces* **9**, 10427–10434 (2017).
31. D. Trefz, A. Ruff, R. Tkachov, M. Wieland, M. Goll, A. Kiriy, S. Ludwigs, Electrochemical investigations of the N-type semiconducting polymer P(NDI2OD-T2) and its monomer: New insights in the reduction behavior. *J. Phys. Chem. C* **40**, 22760–22771 (2015).
32. Y. Suzuki, Y. Kitatsuji, T. Ohnuki, S. Tsujimura, Flavin mononucleotide mediated electron pathway for microbial U(VI) reduction. *Phys. Chem. Chem. Phys.* **12**, 10081–10087 (2010).
33. R. Garjonyte, A. Malinauskas, L. Gorton, Investigation of electrochemical properties of FMN and FAD adsorbed on titanium electrode. *Bioelectrochemistry* **61**, 39–49 (2003).
34. K. Rathee, V. Dhull, R. Dhull, S. Singh, Biosensors based on electrochemical lactate detection: A comprehensive review. *Biochem. Biophys. Rep.* **5**, 35–54 (2016).
35. M. ElMahmoudy, S. Inal, A. Charrier, I. Uguz, G. G. Malliaras, S. Sanaur, Tailoring the electrochemical and mechanical properties of PEDOT:PSS films for bioelectronics. *Macromol. Mater. Eng.* **302**, 1600497 (2017).

Acknowledgments

Funding: A.M.P. and R.M.O. acknowledge the support by the Marie Curie Innovative Training Networks project OrgBio no. 607896. D.O., I.M., and S.I. acknowledge financial support from the King Abdullah University of Science and Technology Office of Sponsored Research (OSR) under award no. OSR-2016-CRG5-3003. A.G. and I.M. acknowledge funding from Engineering and Physical Sciences Research Council Project EP/G037515/1 and EP/N509486/1. **Author contributions:** A.M.P. and D.O. conducted the experiments and prepared the figures. A.G. and I.P.M. provided materials and helped in the preparation of figures. I.U. and J.R. fabricated devices. A.S. performed QCM and AFM experiments. S.I. conceived the research, designed the experiments, and wrote the manuscript with A.M.P. I.M., R.M.O., and S.I. supervised the work. All authors were involved in the discussion and participated in manuscript input and editing. **Competing interests:** A U.S. provisional application (no. 62618794) related to this work was filed by S.I., A.M.P., and A.G. All other authors declare that they have no competing interests. **Data and materials availability:** All data needed to evaluate the conclusions in the paper are present in the paper and/or the Supplementary Materials. Additional data related to this paper may be requested from the authors.

Submitted 23 January 2018
Accepted 8 May 2018
Published 22 June 2018
10.1126/sciadv.aat0911

Citation: A. M. Pappa, D. Ohayon, A. Giovannitti, I. P. Maria, A. Savva, I. Uguz, J. Rivnay, I. McCulloch, R. M. Owens, S. Inal, Direct metabolite detection with an n-type accumulation mode organic electrochemical transistor. *Sci. Adv.* **4**, eaat0911 (2018).

Science Advances

Direct metabolite detection with an n-type accumulation mode organic electrochemical transistor

Anna Maria Pappa, David Ohayon, Alexander Giovannitti, Iuliana Petruta Maria, Achilleas Savva, Ilke Uguz, Jonathan Rivnay, Iain McCulloch, Róisín M. Owens and Sahika Inal

Sci Adv **4** (6), eaat0911.
DOI: 10.1126/sciadv.aat0911